Since January 2020 Elsevier has created a COVID-19 resource centre with free information in English and Mandarin on the novel coronavirus COVID-19. The COVID-19 resource centre is hosted on Elsevier Connect, the company's public news and information website.

Chemical Physics Letters 771 (2021) 138563

Contents lists available at ScienceDirect

Chemical Physics Letters

journal homepage: www.elsevier.com/locate/cplett

Research paper

In silico studies on stilbenolignan analogues as SARS-CoV-2 Mpro inhibitors

Adnan Cetin *

Faculty of Health Sciences, University of Mus Alparslan, Mus 49250, Turkey

ARTICLE INFO

Keywords:
ADMET
COVID-2019
In silico
Gnetifolin F
Docking
Antiviral activity

ABSTRACT

COVID-19, a new strain of coronavirus family, was identified at the end of 2019 in China. The COVID-19 virus spread rapidly all over the world. Scientists strive to find virus-specific antivirals for the treatment of COVID-19. The present study reports a molecular docking study of the stilbenolignans and SARS-CoV-2 main protease (SARS-CoV-2 Mpro) inhibitors. The detailed interactions between the stilbenolignan analogues and SARS-CoV-2 Mpro inhibitors were determined as hydrophobic bonds, hydrogen bonds and electronic bonds, inhibition activity, ligand efficiency, bonding type and distance and etc. The binding energies of the stilbenolignan analogues were obtained from the molecular docking of SARS-CoV-2 Mpro. Lehmbachol D, Maackolin, Gnetucleistol, Gnetifolin F, Gnetofuran A and Aiphanol were found to be −7.7, −8.2, −7.3, −8.5, −8.0 and −7.3 kcal/mol, respectively. Osirus, Molinspiration and SwissADME chemoinformatic tools were used to examine ADMET properties, pharmacokinetic parameters and toxicological characteristics of the stilbenolignan analogues. All analogues obey the Lipinski's rule of five. Furthermore, stilbenolignan analogues were studied to predict their binding affinities against SARS-CoV-2 Mpro using molecular modeling and simulation techniques, and the binding free energy calculations of all complexes were calculated using the molecular mechanics/Poisson–Boltzmann surface area (MM-PBSA) method. With the data presented here it has been observed that these analogues may be a good candidate for SARS-CoV-2 Mpro *in vivo* studies, so more research can be done on stilbenolignan analogues.

1. Introduction

Coronavirus disease 2019 (or COVID-19) emerged worldwide as a threat to public health in Wuhan, is the capital of Hubei Province in the People's Republic of China in late December 2019 [1,2]. The outbreak was initially detected in the seafood and animal markets in Wuhan region. Afterwards, COVID-19 spread from person to person particularly in Wuhan, and then spread to other cities in Hubei province and other provinces of the People's Republic of China and lastly to other world countries [3]. COVID-19 is a virus defined as a result of a research conducted in a group of patients in whom such as fever, cough, shortness of breath were observed on January 13, 2020. COVID-19 was recognized as a pandemic by the World Health Organization (WHO) globally first on March 11, 2020 and WHO named SARS-CoV-2 Mpro pathogen as Severe Acute Respiratory Syndrome CoronaVirus 2 (SARS CoV-2) as a type of coronavirus [4]. No specific effective antiviral therapy for COVID-19 has been found. Although in most COVID-19 patients a mild or moderate course is observed, in up to 5–10% there can be a severe, potentially life-threatening course, and effective medications are urgently needed. Many treatments have been tested including chloroquine, hydroxychloroquine, favipiravir, brincidofovir, lopinavir, ritonavarin, monoclonal antibodies, and plasma of recovering patients against the coronovirus disease [5]. Optimized supportive care continues to be the mainstay of treatment. SARS-CoV-2 Mpro pandemic affects the whole world due to lack of a treatment. This pandemic has caused the death of nearly two and a half million people and still has a fatal effect. Information on treatment for COVID-19 is changing rapidly and there are vaccine studies at the moment. Furthermore, there are approved vaccines in the world and some vaccines have already started to be administered to people [6–9].

Many medicinal plants have been utilized to treat lots of diseases for thousands of years [10,11]. Moreover, these plants have an important role in the production of drug raw materials or new drugs in modern pharmacy since the compounds obtained by these plants constitute the basis in particular of pharmacology [12,13]. Studies on medicinal plants will continue as long as humanity exists since studies on important medicinal plants have contributed to the treatment processes of diseases for many years. It is important to determine the biological activities of

* Corresponding author.
E-mail address: a.cetin@alparslan.edu.tr.

https://doi.org/10.1016/j.cplett.2021.138563
Received 14 January 2021; Received in revised form 17 March 2021; Accepted 18 March 2021
Available online 22 March 2021

these plants, which have not been sufficiently studied as a result of herbal medicines. Stilbenelignans produced by plants is a group of natural products formed from a stilbenoid and a lignan, intersecting moiety of non conventional lignans [14,15]. Stilbenes having an important biologic activity are composed ofa Cinnamoyl-Coenzyme A group and three malonate units. Therefore, these structures formed by the unification of C6-C3 stilbenes with the Cinnamoyl-CoA are regarded as stilbenolignans.

Two phenol structures in stelbenes placed symmetrically along the double bond have been observed and it's hard to distinguish figuring out which one comes from Cinnamoyl-CoA or malonate group has been difficult. It has been seen that hydroxyl moieties in the stilbenolignan structure have different properties such as meta-oriented or orto-oriented because of the different binding sites [16]. Moreover, only six stilbenolignans have been identified in the literature. The stilbenolignans used in this work were found to be from three different plant families. As shown in Fig. 1, Lehmbachol D, Gnetifolin F and Gnetofuran A are identified from *Gnetum cleistostachyum* (Gnetaceae). Maackolin is identified from *Maackia amurensis* (Fabaceae) and, Aiphanol is identified from *Aiphanes aculeata* (Arecaceae). The Stilbenolignans produced from plants are proposed as anti-inflammatory, anti-angiogenic, antioxidant activities for leading compounds in drug discovery. Scientists around the world are actively trying to discover potentially effective drugs that can fight COVID-19 [17,18]. Currently, there are no COVID-19 specific antiviral drugs. Nowadays, the works done on this SARS-CoV-2 Mpro pandemic are very important and scientifically meaningful. Thus, the aim of this study is to determine the molecular docking, molecular modelling studies and pharmacokinetic properties between stilbenolignans analogues and the SARS-CoV-2 Mpro and to investigate their molecular docking results, binding energies and detailed interactions such as binding affinities and the hydrogen, hydrophobic and electronic bonds.

2. Experimental methods

2.1. Docking methodology

The three-dimensional x-ray crystal structure of SARS-CoV-2 Mpro (pdb code: 6LU7) was is retrieved in pdb format from Protein Data Bank with resolution 2.16 Å, respectively [19]. The co-crystallized ligand of the SARS-CoV-2 Mpro (6LU7) structure was extracted. Then, it was prepared in AutodockVina by removal of water and solvent molecules, removal of the bound ligand, addition of polar hydrogens and partial charge assignment and saved as .pdbqt format using AutodockVina to be included as a reference in the virtual screening. The grid box was defined by selecting the co-crystallized inhibitors to keep the center of each docked stilbenolignan analogues with same dimensions of binding box. Moreover, the grid box center was adjusted X = −12.298, Y = 12.598 and Z = 63.594 with dimensions for SARS-CoV-2 Mpro and its size was set to 20x20x20 Angstroms to cover the active site of the SARS-CoV-2 Mpro (6LU7). BIOVIA Discovery Studio software was used molecular modeling visual inspection of docking poses (2D and 3D images) designed for the all complexes [20,21]. The complex structure between the SARS-CoV-2 Mpro and co-crystallized inhibitor of the SARS-CoV-2 Mpro was illustrated in Fig. 2. AutodockVina program was performed between stilbenolignan analogues and SARS-CoV-2 Mpro for molecular docking analysis such as binding types, binding energies, inhibition activities, ligand efficient, distances and possible interactions. Molecular docking scores were set as AutoDock tools of the molecular graphics

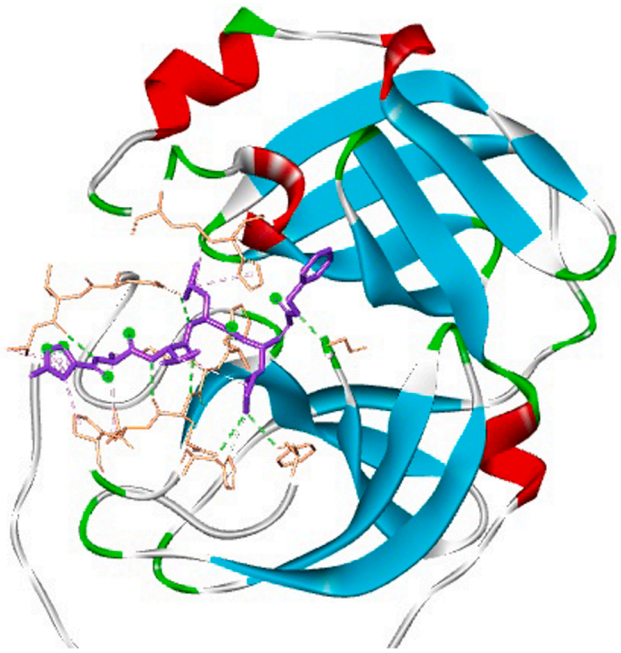

Fig. 2. Complex between SARS-CoV-2 Mpro and its inhibitors.

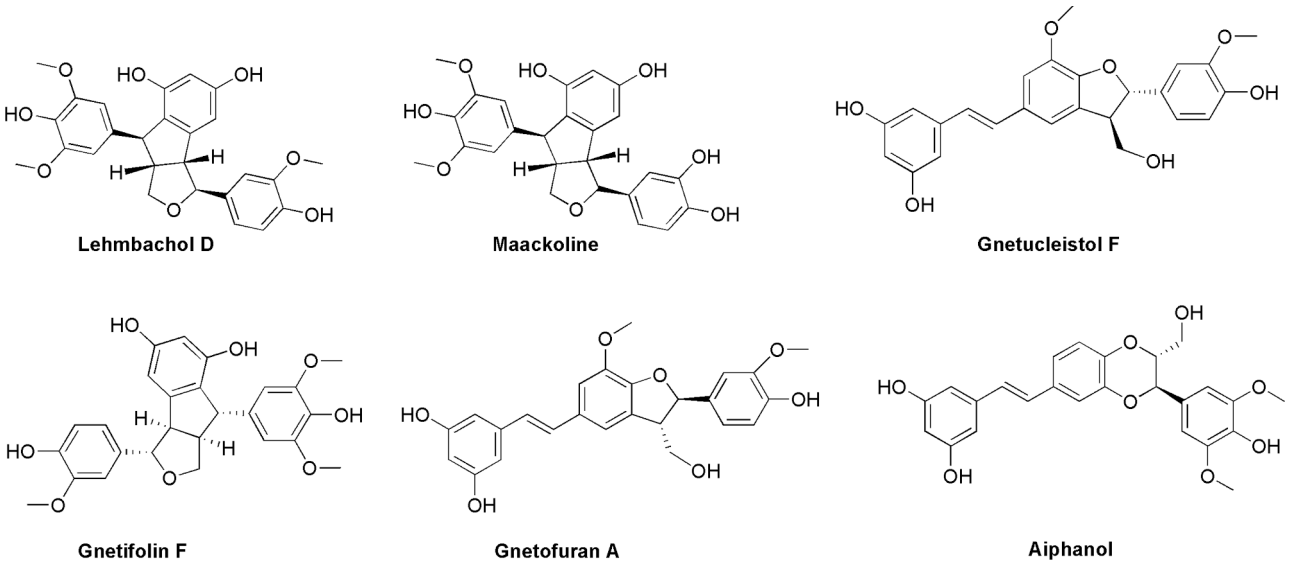

Fig. 1. Structures of stilbenolignans obtained from Gnetaceae, Fabaceae and Arecaceae plants.

laboratory software package by keeping the analogue flexible [22]. Binding Pocket coordinates of the stilbenolignan analogues were employed to define the active site in SARS-CoV-2 Mpro as shown in Fig. 3.

2.2. Osiris/Molinspiration and ADMET analyses

Osiris and Molinspiration analyses are performed to describe 2D models and to indicate the type of pharmacophore site [23]. These analyses are employed to predict pharmacore site and biological activity of the stilbenolignan analogues and also to determine the drug-likeness score, steric effect, electrostatic properties of the stilbenolignan analogues. In addition, these analyses reports key features about the stilbenolignan analogues-SARS-CoV-2 Mpro interactions. The Osiris/Molinspiration parameter values were identified via Cheminformatics free web services (http://www.molinspiration.com/cgi-bin/properties) and (https://www.organic-chemistry.org/prog/peo/). The pharmacokinetic and toxicity properties of the Stilbenolignan analogues were achieved with using the SwissADME which is an open online tool (http://www.swissadme.ch).

The ADME properties define blood-brain barrier (BBB) permeability and passive human gastrointestinal absorption (HIA) as well as substrate or non-substrate permeability glycoprotein (P-gp) and Cytochrome P450 (CYP) [24]. Moreover, SwissADME enables predictions for risks of toxicology such as mutagen test and carcino rat.

Fig. 3. Active site of SARS-CoV-2 Mpro.

2.3. Molecular dynamics and free energy calculation

Molecular dynamic simulations were performed with NAMD 2.12 using Amber ff14SB forcefield and the input files for the simulation are prepared with Amber14 tools [25]. The the SARS-CoV-2 Mpro-stilbenolignan analogues' complexes were solvated using TIP3P water model in cubic water box with at least 12 Å from the each complex to the edge of box. The ion concentration was maintained at 0.15 M and the net charge of system were neutralized by adding 67 Na^+ and 55 Cl^- ions. Langevin dynamics with periodic boundary conditions were applied in the simulation. Van der waals and electrostatic interactions were truncated at 12 Å with a switching function from 10 Å. Particle Mesh Ewald was applied for long-range electrostatic interaction calculations. First, the system underwent a 5000-step minimization with a fixed backbone, and then a subsequent 5000-step minimization without constraint. Then, all atoms in the protein were fixed for 100 ps equilibration of the water. Harmonic constraint of 1 kcal $mol^{-1}\cdot Å^{-2}$ was applied to the SARS-CoV-2 Mpro and stilbenolignan analogues' complexes alpha carbon atoms, and the system was then gradually heated from 0 K to 310 K with 1000- step/K in the canonical ensemble simulation. The system was maintained at 310 K for 1 ns equilibration with alpha carbon atoms constraints and another 2 ns equilibration without constraints in canonical ensemble system. The system was switched to an isothermal-isobaric ensemble simulation and all constraints were removed for the 50 ns production run. Finally, grid box for SARS-CoV-2 Mpro and stilbenolignan analogues' complexes were set exactly identical as for their complex by specifying the grid box size and center [26]. Trajectory analysis, the clusters of ten models of complexes found in the trajectory, RMSD and RMSF values of all the complexes were performed using a Python 2.7 object-oriented package combined with a Fortran-based CABS algorithm implementation [27]. Molecular Mechanics PoissonBoltzmann surface area (MM-PBSA) were computed to understand the binding free energy of the SARS-CoV-2 Mpro-stilbenolignan analogues' complexes for an ensemble (collection/trajectory) of structures. Molecular mechanics-Poisson-Boltzmann surface area (MM-PBSA) is a widely used end point method in free energy calculations [25]. In MM-PBSA, the binding free energy (ΔG_{bind}) of the SARS-CoV-2 Mpro-stilbenolignan analogues' complexes was calculated as the equations below.

$$\Delta G_{\text{MM - PBSA}} = \Delta G_{\text{complex}} - \left(\Delta G_{\text{protein}} + \Delta G_{\text{ligand}}\right)$$

For each molecular dynamic snapshot, the binding free energy of each SARS-CoV-2 Mpro-stilbenolignan analogues' complexes was calculated and the detailed free energy decompositions were performed for all snapshots collected in the sampling phases of molecular dynamic simulations. The Poisson-Boltzmann calculations were performed using the with DelphiForce program [28].

3. Results and discussion

3.1. Molecular docking studies

The stilbenolignans produced from plants are proposed as anti-inflammatory, anti-angiogenic, antioxidant activities for leading compounds in drug discovery [29–31]. Moreover, main interactions between SARS-CoV-2 Mpro and stilbenolignan analogues such as the binding affinities and the hydrogen bonds and the bond lengths etc. were obtained by using Autodock Vina. Also, native ligand as reference ligand, and the recommended drugs for SARS-CoV-2 Mpro treatment; Lopinavir and Nelfinavir were used to compare the molecular docking results of the stilbenolignan analogues [32,33]. The six stilbenolignan analogues formed from some plants were investigated in this study as potential inhibitors of the SARS-CoV-2 Mpro in Fig. 3. Molecular docking is a molecular modeling technique that it is one of the most common methods employed to analyze the detailed interactions

between SARS-CoV-2 Mpro and stilbenolignan analogues. The crystal poses of six stilbenolignan analogues were docked into the binding site of SARS-CoV-2 Mpro with identified docking search algorithms and scoring functions.

All stilbenolignan analogues were docked using similar optimized docking conditions. The native ligand, nelfinavir, lopinavir drugs were identified as shown in Table 1. The binding energy, inhibition activity, ligand efficiency and hydrophobic, hydrogen bonds and electrostatic interactions of stilbenolignan analogues-SARS-CoV-2 Mpro were illustrated in Table 2. Initially, the drug score, Volume A^3 and Surface A^3 were determined for stilbenolignan analogues-SARS-CoV-2 Mpro 0.77, 702.27 and 842.81, respectively. The binding affinity values of stilbenolignan analogues ranged from −8.5 to −7.3 kcal/mol and their ligand effiencies were obtained between −0.21 and −0.25 using Autodock Vina. The binding affinity of Gnetofilin F was found to be −8.5 kkal/mol higher than the value of the reference ligand. The binding affinity of Maackolin was also a very close value as −8.2 kcal/mol. The binding affinities of the Gnetucleistol and Aiphanol analogues (−7.3 kcal/mol) were found lower than those of the other stilbenolignan analogues in this study.

This is thought to be due to the numbered hydroxyl moieties and different structures of the stilbenolignan analogues [12,34]. When the molecular docking results of the stilbenolignan analogues were investigated, all analogues showed alkyl interactions with Cys145, Met165, Pro168, Ala191, Leu50, Leu167, His141, His165, His172 residues in active site in the SARS-CoV-2 Mpro and all analogues except **4** analogue showed π-alkyl interactions with Met165, Leu167, Cys145, and Cys145 residues in the active site of the SARS-CoV-2 Mpro. All analogues except **1** analogue showed hydrophobic bonding type Van der Waals with Phe140, Leu167, Cys145, Gln192, Pro168 and Gln166 residues in the active site of the SARS-CoV-2 Mpro [35]. As shown in Fig. 4 and Table 2, the complex structures between stilbenolignan analogues and the SARS-CoV-2 Mpro were stabilized by hydrogen bonds containing oxygen (-O), hydrogen (-H) and carbonyl (-C═O) moieties simultaneously as donor and acceptor with Cys145, Leu141, Glu166, Arg188, Thr190, Asn142, Gly143, Ser144, His163, Asp148, His164, Gln189, Pro168 [36] and also, the analogue **4** showed π donor hydrogen bond with Pro168 residue in the active site of the SARS-CoV-2 Mpro [37]. Stilbenolignan analogues had electronic interactions with the SARS-CoV-2 Mpro amino acids Glu166, Gln189, Leu167, Cys145, Asp187 and His141 as shown in Table 2. Maackolin included π-anion bond phenyl moiety with the SARS-CoV-2 Mpro amino acid Glu166 at a distance of 4.47 Å (Molecular docking simulations of analogues are given in Supplemantal Materials file).

Gnetucleistol includes π-lone pair bond phenyl moiety with the SARS-CoV-2 Mpro amino acid Glu166 at a distance of 4.52 Å. Gnetifolin F having the highest binding energy includes π-sigma bond with amino acid Gln189 at a distance of 4.21 Å, π-anion with amino acid Glu166 at a distance of 3.69 Å, amide π-stacked with amino acids Leu167 and Cys145 at distances of 4.71 and 4.60 Å. Gnetofuran A includes amide π-stacked with amino acid Asp187 at a distance of 5.14 Å and π-π T-shaped with amino acid His141 at a distance of 6.01 Å. Aiphanol includes amide π-donor hydrogen bond with amino acid Cys145 at a distance of 4.19 Å.

3.2. Pharmacokinetic studies

Osiris and Molinspiration analyses were performed to investigate the pharmacophore features and drug-like properties of the stilbenolignan analogues [38]. The toxicity risk and bioavailability and drug-score properties of the stilbenolignan analogues were calculated using the Osiris Property Explorer in Table 3. The toxicity risk categories can be harmful in the risk category specified [39]. As shown in Table 3, the stilbenolignan analogues did not show mutagenic, tumorigenic, irritative effects. However, Gnetucleistol, Gnetofuran A and Aiphanol analogues showed high toxic effects on the reproduction. The cLogP value which is octanol/water partition coefficient, is calculated by the Osirus Property Explorer and Molinspiration. The cLogP values of the stilbenolignan analogues were found smaller than 5.0 which means these analogues have rational good absorption and permeability. Solubility is a significant parameter for drug design and pharmacology due to the potential absorption and distribution characteristics, so preparing well soluble drugs is always preferred in drug industry [40].

The solubility values of most drugs sold in the market are greater than −4.0 and the solubility values of all stilbenolignan analogues except Gnetucleistol and Gnetofuran A were in the range of −2.90 and −3.58. Their solubility values were also very close to −4; −4.18. Moreover, when the druglikeness values of the stilbenolignan analogues were observed, it was seen that only two analogues had positive values. The drug likeness values of Lehmbachol D and Mackolin were 1.97 and 2.50. Actually, positive value reflects that it contains predominantly fragments frequently present in the commercial drugs [41]. When the log P, H-bond donors, H-bond acceptors and moleculer weight parameters were assessed for the stilbenolignan analogues, it was seen that all analogues obeyed the Lipinski's rule of five. In addition to Osirus calculations, Molinspiration which is a web-based tool, was utilized to predict the bioactivity scores of the stilbenolignan analogues as well as the molecular properties such as moleculer weight, clogP (octanol/water partition coefficient), polar surface area, volume, number of hydrogen bond donor and acceptor etc. as shown in Table 3.

Furthermore, GPCR ligands, ICM, KI, NRL, PI and other EI inhibitors of the stilbenolignan analogues were illustrated with the prediction bioactivity scores using online-site Molinspiration in Table 3. Drug metabolism and pharmacokinetic (ADME) and drug-induced toxicity properties of the stilbenolignan analogues were calculated using SwissADME database as shown in Table 3. The mutagenicity and carcinogeniticy of the stilbenolignan analogues were evaluated using the SwissADME server [42]. The pharmacokinetic and toxicity properties of the Maackolin, Gnetifolin F, Gnetofuran A analogues with high bonding energy were evaluated as these analogues can be potential drug candidates. As seen in Table 3, the transporter class P-glycoprotein (P-gp) and Cytochrome P450 (CYP) metabolic enzymes, which are important in drug metabolism, were assessed in this study. Maackolin analogue was found to be non-inhibitors of all CYPs. Gnetifolin F was found to be non-inhibitors of CYP1A2, CYP2C19, CYP2C9 and CYP2D6 except CYP3A4 inhibitor. Furthermore, Gnetofuran A analogue was found to be

Table 1
Properties of SARS-CoV-2 Mpro inhibitor candidates.

No	Binding Affinity (kcal/mol)	Inhibition Activity (uM)	Ligand Efficiency	Intermole cular Energy	VDW-H Bond Desolvation Energy
Lehmbachol D	−7.7	2.1	−0.23	−10.43	−10.30
Maackolin	−8.2	0.964	−0.25	−10.89	−10.49
Gnetucleistol	−7.3	4.58	−0.21	−10.57	−10.33
Gnetifolin F	−8.5	0.59	−0.27	−10.89	−10.51
Gnetofuran A	−8.0	1.29	−0.25	−11.02	−10.76
Aiphanol	−7.3	4.54	−0.22	−10.27	−9.96
Nelfinavir	−10.7	736.89	−0.27	−14.30	−13.83
Lopinavir	−9.4	126.76	−0.2	−14.18	−13.83
Reference Ligand	−8.3	$13.91x10^{-3}$	−0.17	−14.33	−14.33

Table 2
Molecular docking results and interactions detail of the stilbenolignan analogues.

No	Hydrobophic Bond				Hydrogen Bond			
	Bonding Type	Protein	Ligand	Distance (Å)	Bonding Type	Protein	Ligand	Distance (Å)
		Interacting Amino Acids	Interacting Atoms or Rings			Interacting Amino Acids	Interacting Atoms or Rings	
Lehmbachol D	alkyl	Cys145	-CH_3	4.91	Conventional H bond	Cys145	O	4.75
		Met165	-CH_3	5.62		Leu141	-H	6.76
		Pro168	-CH_3	5.54		Glu166	-H	4.27
		Met:165	-CH_3	4.55		Arg188	-H	5.82
	π-alkyl	Met:165	-Ph	5.88				
		Leu167	-CH_3	3.44				
Maackolin	alkyl	Met165	-Ph	5.96	Conventional H bond	Thr190	-H	4.09
		His163	-CH_3	6.31		Thr190	-H	4.58
		His172	-CH_3	5.25		Arg188	-H	6.00
	π-alkyl	Cys145	-CH_3	4.82		Glu166	-H	4.37
	Van der Waals	Phe140	-CH_3	4.67		Asn142	-H	3.93
						Gly143	-O	3.90
						Cys145	-O	4.82
						Ser144	-O	3.49
						Ser144	-H	3.07
						His163	-O	5.73
					Carbon H bond	Glu166	-O	4.37
					π-anion	Glu166	-Ph	4.47
Gnetucleistol	alkyl	Ala191	-CH_3	4.16	Conventional H bond	Thr190	-O	4.35
		Leu50	-CH_3	4.74		Gly143	-O	4.16
	π-alkyl	Cys145	-Ph	7.09		Leu141	-H	5.24
	Van der Walls	Leu167	-CH_3	6.56		His163	-O	5.41
					π-lone pair	Glu166	-Ph	4.52
Gnetifolin F	alkyl	Pro168	-CH_3	5.87	Conventional H bond	Thr190	-H	4.68
		Met165	-CH_3	5.34		Glu166	-H	4.15
	Van der Waals	Cys145	-Ph	6.74		Asn142	-H	4.03
						Gly143	-O	3.80
						Gly143	-O	3.53
						Leu141	-H	6.51
						Ser144	-H	2.45
					π-donor hydrogen bond	Pro168	-O	4.97
					π-sigma	Gln189	-Ph	4.21
					π-anion	Glu166	-Ph	3.69
					Amide-πstacked	Leu167	-CH_3	4.70
						Cys145	-CH_3	4.61
Gnetofuran A	alkyl	Pro168	-CH_3	4.84	Conventional H bond	Glu166	-H	4.95
		Leu167	-CH_3	4.70		Asp187	-H	4.60
	π-alkyl	Pro168	-Ph	4.24		His164	-H	3.33
		Met165	-Ph	6.55	Amide-π stacked	Asp187	-Ph	5.14
		Met165	-Ph	4.98	π-π T-Shaped	His41	-Ph	6.01
	Van der Waals	Gln192	-CH_3	2.87				
		Pro168	-O	4.27				
Aiphanol	alkyl	His172	-CH_3	5.26	Conventional H bond	His163	-O	5.44
		His163	-CH_3	6.18		Ser144	-H	2.64
		Cys145	-CH_3	4.74		Leu141	-H	5.79
		His141	-CH_3	5.82		Cys145	-O	4.19
	π-alkyl	Pro168	-Ph	4.25		Gln189	-H	3.85
		Met165	-Heg	4.72		Pro168	-H	6.16
	Van der Waals	Glu166	-CH_3	4.01	π-donor hydrogen bond	Cys145	-Ph	4.19

inhibitors of CYP2C9, CYP2D6 and CYP3A4. The CYP inhibitors of the these analogues are significant to explore the pharmacokinetics for preventing undesired drug-drug interactions and also, Gnetofuran A having P-gp and CYP3A4 can be a barrier in the transmembrane transportation of drugs since both are good transporters in the intestine [43].

In addition to pharmacokinetic properties, the inhibition constant values of these analogues are compatible with their binding affinities. Gnetifolin F analogue had the lowest inhibition constant value with 6.73 nM in the stilbenolignan analogues. Besides, Gnetifolin F was found inhibition constant with 0.59 nM as result of molecular docking of the Gnetifolin F-SARS-CoV-2 Mpro. It was observed that these analogues obtained good results in terms of their toxicity properties for Ames mutagenicity test from SwissADME database.

3.3. Molecular dynamics simulations

All SARS-CoV-2 Mpro-stilbenolignan analogues' complexes were subjected for subsequent molecular dynamics and free energy calculation due to investigate the dynamic stability of the SARS-CoV-2-inhibitor complexes. The root mean-square deviations (RMSDs) and root mean square fluctuations (RMSFs) of the Cα atoms for the each complex were calculated by the CABS-flex web server. RMDSs and RMSFs were plotted for SARS-CoV-2 Mpro-stilbenolignan analogues' complexes that converged during the 50 ns MD simulation in Figs. 5 and 6 [44]. It was observed that all complexes induced flexibility to some residues in the SARS-CoV-2 Mpro. The highest fluctuations were observed in several regions, ranging from 54 to 59 for Lehmbachol D and Gnetifolin F analogues, 145–150 for Maackolin and Gnetifolin F analogues, 163–168 for Aiphanol analogue (See Supplemantal Materials

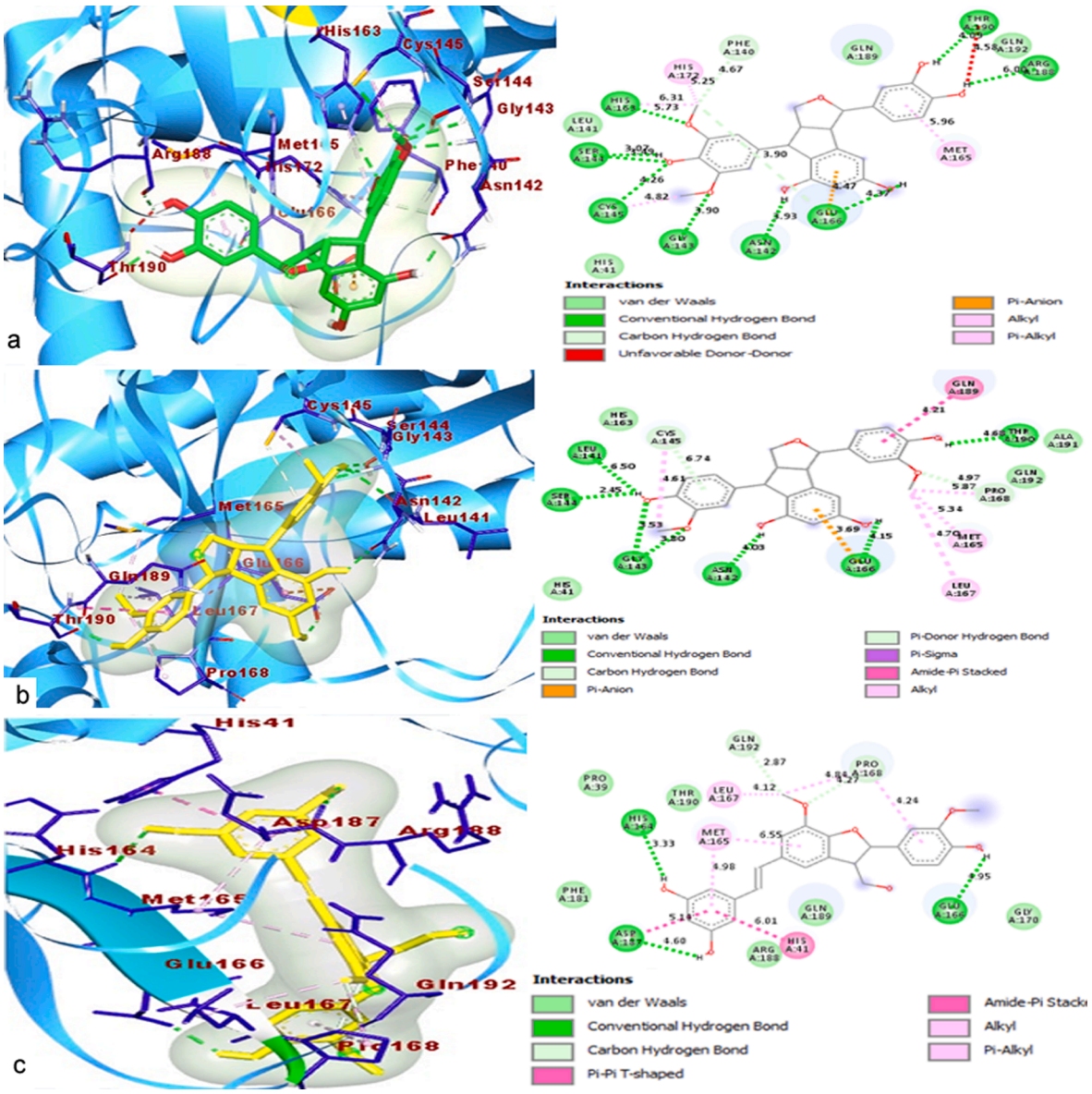

Fig. 4. All types of interactions between stilbenolignan analogues and SARS-CoV-2 Mpro.

file).

All complexes were are almost more fluctuated during the simulation in loop region. The superimpose analysis of the receptor binding domains were carried separately for SARS-CoV-2 Mpro-stilbenolignan analogues' complexes. As the Gnetifolin F analogue showed the highest binding affinity, superimposed structure of SARS-CoV-2 Mpro-Gnetifolin F complex was depicted in Fig. 7. Initial and last confirmation of the dynamics trajectory of the all complexes were analyzed using the Pymol software [45]. RMSD values of the SARS-CoV-2 Mpro-stilbenolignan analogues' complexes (Lehmbachol D, Maackolin, Gnetucleistol, Gnetifolin F, Gnetofuran A and Aiphanol) were found to be 2.127, 1.839, 1.483, 1.668, 1.792 and 1.684, respectively.

The binding free energies the SARS-CoV-2 Mpro-stilbenolignan analogues' complexes were calculated for molecular dynamic snapshots and the MM-PBSA calculations of all complexes were performed using the Delphi web server [46–47]. The binding free energy values from the MM-PBSA calculation of the SARS-CoV-2 Mpro-stilbenolignan analogues' complexes were reported in Table 4.

The results indicated that SARS-CoV-2 Mpro-Maackolin complex possessed highest negative binding free energy value of −103.61 kJ/mol followed by SARS-CoV-2 Mpro-Gnetifolin F complex with value of −99.59 kJ/mol. SARS-CoV-2 Mpro-Gnetofuran A complex showed close affinity with value of −97.54 kJ/mol. SARS-CoV-2 Mpro-Lehmbachol D and SARS-CoV-2 Mpro-Aiphanol complexes showed lowest affinity with values of −91.25 and −92.31 kJ/mol. The nature of interactions of Glu, His, Phe140 residues of the SARS-CoV-2 Mpro-Maackoline complex were observed as hydrogen bonding and Van der Waals hydrophobic bonding type. Moreover, the SARS-CoV-2 Mpro-Gnetifolin F complex had same interactions as well as π-donor, π-sigma, π-anion bonding types. However, the interactions of the SARS-CoV-2 Mpro-Lehmbachol D and the SARS-CoV-2 Mpro-Aiphanol complexes are less. Furthermore, some residues of SARS-CoV-2 Mpro contributed with small negative binding energies were determined such as Met165, Cys145 and Pro168. MM-PBSA results of the SARS-CoV-2 Mpro-stilbenolignan analogues' complexes revealed that hydrophobic and hydrogen bonding interactions which govern changes in bonding properties of the stilbenolignan analogues to residues of SARS-CoV-2 Mpro. The finding results were compared to the latest researches which is focused on MM-PBSA binding energy calculations of the drugs used against SARS-CoV-2 Mpro [48,49]. It was observed that the important binding site residues

Table 3
Drug likeliness properties of the stilbenolignan analogues by some web tools.[a,b,c]

Drug likeness properties	Lehmbachol D	Maackolin	Gnetucleistol	Gnetifolin F	Gnetofuran A	Aiphanol
Bioavailability and drug-score[a]						
Molecular weight g/mol	466.0	452.0	436.0	466.0	436.0	452.0
cLogP	3.17	2.90	4.18	3.17	4.18	3.58
Solubility	−3.55	−3.23	−4.22	−3.55	−4.22	−4.05
TPSA	117.8	128.8	108.6	117.8	108.6	117.8
Druglikeness	1.97	2.50	−0.55	−4.81	−0.55	−0.49
Drug-score	0.77	0.77	0.77	0.77	0.77	0.77
Toxicity risks[a]						
Mutagenic	nt	nt	nt	nt	nt	nt
Tumorigenic	nt	nt	nt	nt	nt	nt
Irritant	nt	nt	nt	nt	nt	nt
Reproductive effective	nt	nt	ht	nt	ht	ht
Druglikeness[b]						
GPCR ligand	0.20	0.21	0.29	0.19	0.29	0.14
Ion channel modulator	−0.07	−0.07	−0.11	−0.08	−0.11	−0.02
Kinase inhibitor	−0.08	−0.09	−0.05	−0.10	−0.05	−0.13
Nuclear receptor ligand	0.13	0.13	0.08	0.12	0.08	0.22
Protease inhibitors	−0.02	−0.02	−0.16	−0.01	−0.16	0.02
Enzyme inhibitor	0.08	0.08	0.35	0.07	0.35	0.23
Pharmacokinetics[c]						
Ames_test	–	Non-mutagen	–	Non-mutagen	Non-mutagen	–
Carcino_Rat	–	Negative	–	Negative	Negative	–
BBB permeant	–	no	–	no	no	–
GI absorption	–	high	–	high	high	–
P-gp	–	yes	–	no	yes	–
Inhibition Constant nM)	–	7.26	–	6.73	6.75	–
1A2	–	no	–	no	no	–
2C19	–	no	–	no	no	–
2C9	–	no	–	no	yes	–
2D6	–	no	–	no	yes	–
3A4	–	no	–	yes	yes	–

nt = not toxic; ht = high toxic; GI:Gastrointestinal absorption; BBB: Blood brain barrier; P-gp:Permeability Glycoprotein; CYP: Cytochrome P450; a = Osiris; b = Molinspiration; c = SwissAdme.

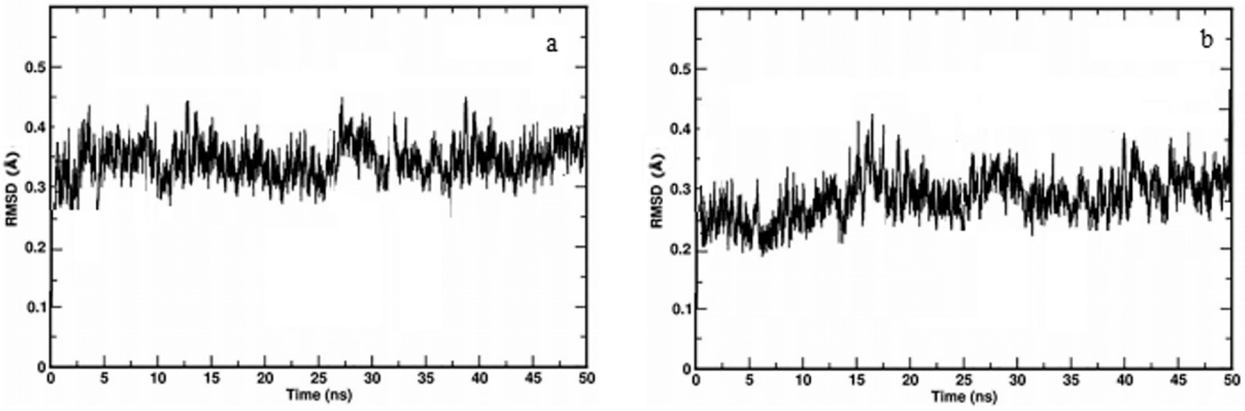

Fig. 5. RMDS plots of the a) SARS-CoV-2 Mpro-Gnetifolin F b) SARS-CoV-2 Mpro-Maackolin analogues complexes.

Met165, Cys145, Pro168, Phe140, Asp187, Thr190, His163, Arg188, Gly143, Leu167 and Glu143 reported was same with residues identified in this study. Furthermore, all SARS-CoV-2 Mpro-stilbenolignan analogues' complexes as binding energy were found to be better than many repurposing inhibitors against SARS-CoV-2 Mpro [50]. The MM-PBSA results of the SARS-CoV-2 Mpro-stilbenolignan analogues' complexes were an significant clue and these stilbenolignan analogues can be a strong inhibitory for SARS-CoV-2 Mpro. The significant key residues were found to be Met165, Glu166, Leu141, Phe140 and His163. The MM-PBSA binding free energy results show that all stilbenolignan analogues may act as a lead compound for clinical drug against SARS-CoV-2 Mpro.

4. Conclusions

In conclusion, this study revealed molecular interaction analyses of docking and ADMET properties between SARS-CoV-2 Mpro and the stilbenolignan analogues. The molecular docking simulations of the stilbenolignan analogues-SARS-CoV-2 Mpro revealed to show similar binding conformations. As result of the molecular interaction analyses of Gnetifolin F, the binding affinity was found to be −8.5 (kcal/mol) with the residues of Glu166 and it was observed that Gnetifolin F can be a strong inhibitor candidate. A stable conformer and good binding site occurred by creating aromatic, hydrogen and hydrophobic bonds in the SARS-CoV-2 Mpro active site residues such as Pro168, Met165, Cys145, Thr190, Glu166, Asn142, Gly143, Leu141, Ser144. In addition, π-donor hydrogen bond interaction with the residue of Pro168, π-sigma interaction with the residue of Gln189, π-anion interaction with the residue

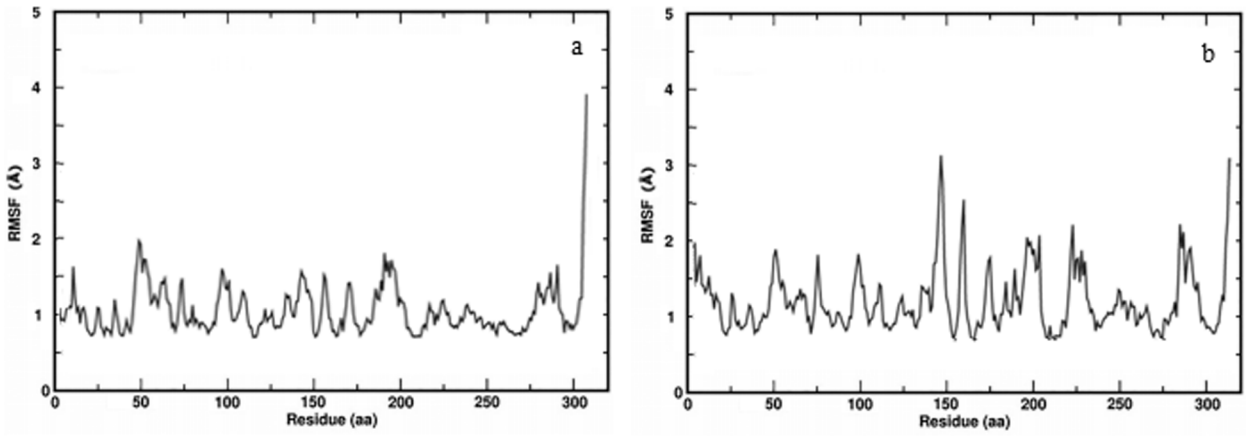

Fig. 6. RMSF plots of the a) SARS-CoV-2 Mpro-Gnetifolin F b) SARS-CoV-2 Mpro-Maackolin analogues complexes.

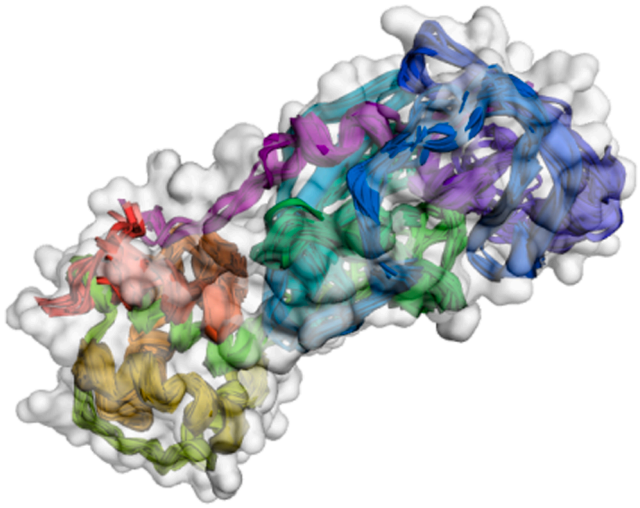

Fig. 7. The superimposed structure of SARS-CoV-2 Mpro-Gnetifolin F complex with the 3Dmol Server.

Table 4
MM-PBSA energy values of complexes between SARS-CoV-2 Mpro and the stilbenolignan analogues.

No	Complex	Binding energy (kJ/mol)	Hotspot interaction binding energy (kcal/mol)
1	SARS-CoV-2 Mpro-Lehmbachol D	−91.25 ± 1.93	−3.35
2	SARS-CoV-2 Mpro-Maackolin	−103.61 ± 2.40	−5.41
3	SARS-CoV-2 Mpro-Gnetucleistol	−96.68 ± 2.56	−4.37
4	SARS-CoV-2 Mpro-Gnetifolin F	−99.59 ± 1.90	−4.98
5	SARS-CoV-2 Mpro-Gnetofuran A	−97.54 ± 3.67	−4.10
6	SARS-CoV-2 Mpro-Aiphanol	−92.31 ± 3.56	−3.82

of Glu166 and amide-π stacked interaction with the residue of Cys145 played an important role in the Gnetifolin F analogue-SARS-CoV-2 Mpro binding. Moreover, the results of ADMET and pharmacokinetic analyses suggested that stilbenolignan analogues were consonant with the many accepted rules and the criteria of drug-likeness. Besides, the toxicity results of the SwissADME suggest that Maackolin, Gnetifolin F and Gnetofuran A analogues were nonmutagenic and noncarcinogenic and also these analogues might have potential activity in the SARS-CoV-2 disease due to good binding energy and pharmacokinetic properties. Moreover, as result of binding free energy calculations, SARS-CoV-2 Mpro-Maackolin analogue complex showed the highest negative binding free energy value of −103.61 kJ/mol, followed by SARS-CoV-2 Mpro-Gnetifolin F analogue complex with value of −99.59 kJ/mol. It was observed that all SARS-CoV-2-stilbenolignan analogues' complexes had close values for binding free energy. Analysis of the molecular dynamic trajectory and MM-PBSA results revealed that all stilbenolignan analogues with SARS-CoV-2 Mpro showed good binding with key residues towards COVID-19 targets. Therefore, it can be considered that the *in vitro* and *in vivo* studies of these analogues can be done in detail as drug candidates against SARS-CoV-2 disease. The stilbenolignan analogues might be suitable drugs for medical applications in drug industry.

CRediT authorship contribution statement

Adnan Cetin: Conceptualization, Methodology, Software, Validation, Data curation, Writing - review & editing.

Declaration of Competing Interest

The authors declare that they have no known competing financial interests or personal relationships that could have appeared to influence the work reported in this paper.

Appendix A. Supplementary material

Supplementary data to this article can be found online at https://doi.org/10.1016/j.cplett.2021.138563.

References

[1] J. Zheng, SARS-CoV-2: an emerging coronavirus that causes a global threat, Int. J. Biol. Sci. 16 (10) (2020) 1678–1685, https://doi.org/10.7150/ijbs.45053.
[2] D. Fisher, D. Heymann, Q&A: The novel coronavirus outbreak causing COVID-19, BMC Med. 18 (1) (2020) 1–3, https://doi.org/10.1186/s12916-020-01533-w.
[3] Y. Yan, W.I. Shin, Y.X. Pang, Y. Meng, J. Lai, C. You, C.H. Pang, The first 75 days of novel coronavirus (SARS-CoV-2) outbreak: recent advances, prevention, and treatment, Int. J. Environ. Res. Public Health 17 (7) (2020) 2301–2323, https://doi.org/10.3390/ijerph17072323.
[4] S. Khaerunnisa, H. Kurniawan, R. Awaluddin, S. Suhartati, S. Soetjipto, Potential inhibitor of COVID-19 main protease (Mpro) from several medicinal plant compounds by molecular docking study. Prepr 20944 (2020) 1–14. https://doi: 10.20944/preprints202003.0226.v1.
[5] H. Lu, Drug treatment options for the 2019-new coronavirus (2019-nCoV), Biosci. Trends 14 (1) (2020) 69–71, https://doi.org/10.5582/bst.2020.01020.
[6] J.V. Lazarus, S.C. Ratzan, A. Palayew, L.O. Gostin, H.J. Larson, K. Rabin, A. El-Mohandes, A global survey of potential acceptance of a COVID-19 vaccine, Nat. Med. (2020) 1–4, https://doi.org/10.1038/s41591-020-1124-9.

[7] N.N. Zhang, X.F. Li, Y.Q. Deng, H. Zhao, Y.J. Huang, G. Yang, Y. Guo, A thermostable mRNA vaccine against COVID-19, Cell 182 (5) (2020) 1271–1283, https://doi.org/10.1016/j.cell.2020.07.024.

[8] J.H. Tanne, Covid-19: FDA panel votes to approve Pfizer BioNTech vaccine (2020) 1. https://doi.org/10.1136/bmj.m4799.

[9] E. Mahase, Covid-19: Moderna applies for US and EU approval as vaccine trial reports 94.1% efficacy, Br. Med. J. 371 (2020) 1, https://doi.org/10.1136/bmj.m4709.

[10] B.B. Petrovska, Historical review of medicinal plants' usage, Pharmacogn. Rev. 6 (11) (2012) 1, https://doi.org/10.4103/0973-7847.95849.

[11] R.A. Oluwafemi, I. Olawale, J.O. Alagbe, Recent trends in the utilization of medicinal plants as growth promoters in poultry nutrition-a review, Res Agri Vet Sci 4 (1) (2020) 5–11.

[12] B.E. Van Wyk, M. Wink, Medicinal plants of the world, CABI. (2018) 381.

[13] M. Saxena, J. Saxena, R. Nema, D. Singh, A. Gupta, Phytochemistry of medicinal plants, J. Pharmacogn. Phytochem. 1 (6) (2013) 168–182.

[14] A. Cassidy, B. Hanley, R.M. Lamuela-Raventos, Isoflavones, lignans and stilbenes–origins, metabolism and potential importance to human health, J. Sci. Food Agric. 80 (7) (2000) 1044–1062, https://doi.org/10.1002/(SICI)1097-0010(20000515)80:7<1044::AID-JSFA586>3.0.CO;2-N.

[15] A. Tsopmo, F.M. Awah, Kuete, V. Lignans, and stilbenes from African medicinal plants, in: Medicinal plant research in Africa Elsevier, 2013, pp. 473–478.

[16] S.A. Begum, M. Sahai, A.B. Ray, Non-conventional lignans: coumarinolignans, flavonolignans, and stilbenolignans. In Fortschritte der Chemie organischer Naturstoffe/Progress in the Chemistry of Organic Natural Products, Springer, Vienna. 93 (2010) 1–70.

[17] W.J. Wiersinga, A. Rhodes, A.C. Cheng, S.J. Peacock, H.C. Prescott, Pathophysiology, transmission, diagnosis, and treatment of coronavirus disease 2019 (COVID-19): a review, JAMA 324 (8) (2020) 782–793.

[18] A. Cortegiani, G. Ingoglia, M. Ippolito, A. Giarratano, S. Einav, A systematic review on the efficacy and safety of chloroquine for the treatment of COVID-19, J. Critical Car 57 (2020) 279–283, https://doi.org/10.1016/j.jcrc.2020.03.005.

[19] Z. Xu, C. Peng, Y. Shi, Z. Zhu, K. Mu, X. Wang, W. Zhu, Nelfinavir was predicted to be a potential inhibitor of 2019-nCov main protease by an integrative approach combining homology modelling, molecular docking and binding free energy calculation, BioRxiv (2020), https://doi.org/10.1101/2020.01.27.921627.

[20] P. Rao, A. Shukla, P. Parmar, R.M. Rawal, B. Patel, M. Saraf, D. Goswami, Reckoning a fungal metabolite, Pyranonigrin A as a potential Main protease (Mpro) inhibitor of novel SARS-CoV-2 virus identified using docking and molecular dynamics simulation, Biophys. Chem. 264 (2020), 106425, https://doi.org/10.1016/j.bpc.2020.106425.

[21] R. Hatada, K. Okuwaki, Y. Mochizuki, Y. Handa, K. Fukuzawa, Y. Komeiji, S. Tanaka, Fragment molecular orbital based interaction analyses on COVID-19 main protease-inhibitor N3 complex (PDB ID: 6LU7), J. ChemistryInf Model 60 (7) (2020) 3593–3602, https://doi.org/10.1021/acs.jcim.0c00283.

[22] D. Seeliger, B.L. de Groot, Ligand docking and binding site analysis with PyMOL and Autodock/Vina, J. Comput. Aided Mol. Des. 24 (5) (2010) 417–422, https://doi.org/10.1007/s10822-010-9352-6.

[23] K.O. Rachedi, T.S. Ouk, R. Bahadi, A. Bouzina, S.E. Djouad, K. Bechlem, M. Berredjem, Synthesis, DFT and POM analyses of cytotoxicity activity of α-amidophosphonates derivatives: Identification of potential antiviral O O-pharmacophore site, J. Mol. Struct. 1197 (2019) 196–203, https://doi.org/10.1016/j.molstruc.2019.07.053.

[24] A. Daina, O. Michielin, V. Zoete, SwissADME: a free web tool to evaluate pharmacokinetics, drug-likeness and medicinal chemistry friendliness of small molecules, Sci. Rep. 7 (2017) 42717, https://doi.org/10.1038/srep42717.

[25] B. Ji, S. Liu, X. He, V.H. Man, X.Q. Xie, J. Wang, Prediction of the binding affinities and selectivity for CB1 and CB2 ligands using homology modeling, molecular docking, molecular dynamics simulations, and MM-PBSA binding free energy calculations, ACS Chem. Neurosci. 11 (8) (2020) 1139–1158, https://doi.org/10.1021/acschemneuro.9b00696.

[26] T. Hazra, S.A. Ullah, S. Wang, E. Alexov, S. Zhao, A super-Gaussian Poisson-Boltzmann model for electrostatic free energy calculation: smooth dielectric distribution for protein cavities and in both water and vacuum states, J. Math. Biol. 79 (2) (2019) 631–672, https://doi.org/10.1007/s00285-019-01372-1.

[27] A. Kuriata, A.M. Gierut, T. Oleniecki, M.P. Ciemny, A. Kolinski, M. Kurcinski, S. Kmiecik, CABS-flex 2.0: a web server for fast simulations of flexibility of protein structures. Nucleic Acids Res 46(W1) (2018) W338-W343. https://doi.org/10.1093/nar/gky356.

[28] M. Petukh, M. Li, E. Alexov, Predicting binding free energy change caused by point mutations with knowledge-modified MM/PBSA method, PLoS Comput. Biol. 11 (7) (2015), e1004276, https://doi.org/10.1371/journal.pcbi.1004276.

[29] C.S. Yao, M. Lin, L. Wang, Isolation and biomimetic synthesis of anti-inflammatory stilbenolignans from Gnetum cleistostachyum, Chem. Pharm. Bull. 54 (7) (2006) 1053–1057, https://doi.org/10.1248/cpb.54.1053.

[30] D. Lee, M. Cuendet, J.S. Vigo, J.G. Graham, F. Cabieses, H.H. Fong, A.D. Kinghorn, A novel cyclooxygenase-inhibitory stilbenolignan from the seeds of Aiphanes aculeata, Org. Lett. 3 (14) (2001) 2169–2171, https://doi.org/10.1021/ol015985j.

[31] N.I. Kulesh, N.A. Vasilevskaya, M.V. Veselova, V.A. Denisenko, S.A. Fedoreev, Minor polyphenols from Maackia amurensis wood, Chem. Nat. Compd. 44 (6) (2008) 712–714, https://doi.org/10.1007/s10600-009-9195-3.

[32] B. Cao, Y. Wang, D. Wen, W. Liu, J. Wang, G. Fan, X. Li, A trial of lopinavir–ritonavir in adults hospitalized with severe Covid-19, N. Eng. J. Med. 382 (2020) 1787–1799, https://doi.org/10.1056/NEJMoa2001282.

[33] B.R. Beck, B. Shin, Y. Choi, S. Park, K. Kang, Predicting commercially available antiviral drugs that may act on the novel coronavirus (SARS-CoV-2) through a drug-target interaction deep learning model, Comput. Struct. Biotechnol. J. 18 (2020) 784–790, https://doi.org/10.1016/j.csbj.2020.03.025.

[34] J.T. Muya, D.T. Mwanangombo, P.V. Tsalu, P.T. Mpiana, D.S.T. Tshibangu, H. Chung, Conceptual DFT study of the chemical reactivity of four natural products with anti-sickling activity, SN Appl. Sci. 1 (11) (2019) 1457, https://doi.org/10.1007/s42452-019-1438-8.

[35] C. Qin, X. Hu, B. Yang, J. Liu, Y. Gao, Amino, nitro, chloro, hydroxyl and methyl substitutions may inhibit the binding of PAHs with DNA, Environ. Pollut. 268 (2020), 115798, https://doi.org/10.1016/j.envpol.2020.115798.

[36] P.T. Mpiana, D.S. Tshibangu, J.T. Kilembe, B.Z. Gbolo, D.T. Mwanangombo, C. L. Inkoto, D.D. Tshilanda, Identification of potential inhibitors of SARS-CoV-2 main protease from Aloe vera compounds: a molecular docking study, Chem. Phys. Lett. 754 (2020), 137751, https://doi.org/10.1016/j.cplett.2020.137751.

[37] C. Trujillo, G. Sánchez-Sanz, A study of π–π stacking interactions and aromaticity in polycyclic aromatic hydrocarbon/nucleobase complexes, ChemPhysChem 17 (3) (2016) 395–405, https://doi.org/10.1002/cphc.201501019.

[38] U.D. Uysal, D. Ercengiz, O. Karaosmanoğlu, B. Berber, H. Sivas, H. Berber, Theoretical and experimental electronic transition behaviour study of 2-((4-(dimethylamino) benzylidene) amino)-4-methylphenol and its cytotoxicity, J. Mol. Struct. 1227 (2020), 129370, https://doi.org/10.1016/j.molstruc.2020.129370.

[39] M. Rashid, Design, synthesis and ADMET prediction of bis-benzimidazole as anticancer agent, Bioorg. Chem. 96 (2020), 103576, https://doi.org/10.1016/j.bioorg.2020.103576.

[40] A.K. Ramalingam, S.G.A. Selvi, V.P. Jayaseelan, Targeting prolyl tripeptidyl peptidase from Porphyromonas gingivalis with the bioactive compounds from Rosmarinus officinalis, Asian Biomed. 13 (5) (2020) 197–203, https://doi.org/10.1515/abm-2019-0061.

[41] M.A. da Silva, M.P. Veloso, K. de Souza Reis, G. de Matos Passarini, A.P.D.A. dos Santos, L. do Nascimento Martinez, C.C. Kuehn, In silico evaluation and in vitro growth inhibition of Plasmodium falciparum by natural amides and synthetic analogs. Parasitol Res 119 (2020) 1879–1887. https://doi.org/10.1007/s00436-020-06681-9.

[42] P. Chowdhury, In silico investigation of phytoconstituents from Indian medicinal herb 'Tinospora cordifolia (giloy)'against SARS-CoV-2 (COVID-19) by molecular dynamics approach, J. Biomol. Struct. Dyn. (2020) 1–18, https://doi.org/10.1080/07391102.2020.1803968.

[43] G.Y. Wang, H.H. Zheng, K.Y. Zhang, F. Yang, T. Kong, B. Zhou, S.X. Jiang, The roles of cytochrome P450 and P-glycoprotein in the pharmacokinetics of florfenicol in chickens, Iran J. Vet. Res. 19 (1) (2018) 9–14.

[44] M. Kurcinski, T. Oleniecki, M.P. Ciemny, A. Kuriata, A. Kolinski, S. Kmiecik, CABS-flex standalone: a simulation environment for fast modeling of protein flexibility, Bioinformatics 35 (4) (2019) 694–695, https://doi.org/10.1093/bioinformatics/bty685.

[45] K.L. Damm, H.A. Carlson, Gaussian-weighted RMSD superposition of proteins: a structural comparison for flexible proteins and predicted protein structures, Biophys. J . 90 (12) (2006) 4558–4573, https://doi.org/10.1529/biophysj.105.066654.

[46] W. Rocchia, E. Alexov, B. Honig, Extending the applicability of the nonlinear poisson-Boltzmann equation: multiple dielectric constants and multivalent ions, J. Phys. Chem. B 105 (28) (2001) 6507–6514, https://doi.org/10.1021/jp010454y.

[47] L. Li, A. Chakravorty, E. Alexov, DelPhiForce, a tool for electrostatic force calculations: applications to macromolecular binding, J. Comput. Chem. 38 (9) (2017) 584–593, https://doi.org/10.1002/jcc.24715.

[48] J.K. Varughese, K.L. Joseph Libin, K.S. Sindhu, A.V. Rosily, T.G. Abi, Investigation of the inhibitory activity of some dietary bioactive flavonoids against SARS-CoV-2 using molecular dynamics simulations and MM-PBSA calculations, J. Biomol. Struct. Dyn. (2021) 1–16, https://doi.org/10.1080/07391102.2021.1891139.

[49] P. Sang, S.H. Tian, Z.H. Meng, L.Q. Yang, Anti-HIV drug repurposing against SARS-CoV-2, RSC Adv. 10 (27) (2020) 15775–15783, https://doi.org/10.1039/D0RA01899F.

[50] Baby, S. Maity, C.H. Mehta, A. Suresh, U.Y. Nayak, Y. Nayak, Targeting SARS-CoV-2 main protease: a computational drug repurposing study, Arch. Med. Res. 52 (1) (2021) 38–47, https://doi.org/10.1016/j.arcmed.2020.09.013.